Biogeosciences, 22, 4333–4347, 2025
https://doi.org/10.5194/bg-22-4333-2025

Biogeosciences Open Access EGU

Triple oxygen isotope evidence for the pathway of nitrous oxide production in a forested soil with increased emission on rainy days

Weitian Ding[1,2], Urumu Tsunogai[1], Tianzheng Huang[1], Takashi Sambuichi[1], Wenhua Ruan[1], Masanori Ito[1], Hao Xu[1], Yongwon Kim[3], and Fumiko Nakagawa[1]

[1]Graduate School of Environmental Studies, Nagoya University, Furo-cho, Chikusa-ku, Nagoya 464-8601, Japan
[2]School of Resources & Environment, Nanchang University, Nanchang 330031, China
[3]International Arctic Research Center, University of Alaska Fairbanks, Fairbanks, Alaska 99775-7320, USA

Correspondence: Weitian Ding (dingweitian@ncu.edu.cn)

Received: 2 March 2025 – Discussion started: 28 March 2025
Revised: 14 June 2025 – Accepted: 16 June 2025 – Published: 1 September 2025

Abstract. Continuous increases in atmospheric nitrous oxide (N_2O) concentrations are a global concern. Both nitrification and denitrification are the major pathways of N_2O production in soil, one of the most important sources of tropospheric N_2O. The ^{17}O excess ($\Delta^{17}O$) of N_2O can be a promising signature for identifying the main pathway of N_2O production in soil. However, reports on $\Delta^{17}O$ are limited. Thus, we determined temporal variations in the $\Delta^{17}O$ of N_2O emitted from forested soil for more than one year and that of soil nitrite (NO_2^-), which is a possible source of O atoms in N_2O. We found that N_2O emitted from the soil exhibited significantly higher $\Delta^{17}O$ values on rainy days ($+0.12 \pm 0.13$ ‰) than on fine days (-0.30 ± 0.09 ‰), and the emission flux of N_2O was significantly higher on rainy days (38.8 ± 28.0 µg $N\,m^{-2}\,h^{-1}$) than on fine days (3.8 ± 3.1 µg $N\,m^{-2}\,h^{-1}$). Because the $\Delta^{17}O$ values of N_2O emitted on rainy and fine days were close to those of soil NO_2^- ($+0.23 \pm 0.12$ ‰) and O_2 (-0.44 ‰), we concluded that although nitrification was the main pathway of N_2O production in the soil on fine days, denitrification became active on rainy days, resulting in a significant increase in the emission flux of N_2O. This study reveals that the main pathway of N_2O production can be identified by precisely determining the $\Delta^{17}O$ values of N_2O emission from soil and by comparing the $\Delta^{17}O$ values with those of NO_2^-, O_2, and H_2O in the soil.

1 Introduction

Nitrous oxide (N_2O) is a strong greenhouse gas and an essential substance in stratospheric ozone depletion (Dickinson and Cicerone, 1986). Since pre-industrial times, the atmospheric N_2O level has increased by 24 % to 335.8 ppb, with an average growth rate of 1.05 ppb yr^{-1} in the last decade (WMO, 2023). Terrestrial soils account for approximately 60 % of total N_2O emissions (Tian et al., 2020). Therefore, better knowledge of the pathways of N_2O production in soils is required to establish mitigation measures.

Both nitrification and denitrification are representative microbial pathways of N_2O production in soils (Wrage et al., 2001). Nitrification is the oxidation of ammonium (NH_4^+) to nitrate (NO_3^-) via aerobic microbial activity, during which N_2O is produced as a byproduct of hydroxylamine (NH_2OH) oxidation to nitrite (NO_2^-), while denitrification is the reduction of NO_3^- to NO_2^- and then to N_2O which is further reduced to nitrogen (N_2) via facultative anaerobes (Fig. 1). Soil conditions such as moisture content, O_2 availability (Bateman and Baggs, 2005; Zhu et al., 2013), temperature (Luo et al., 2007), and fertilizer types (Zhu et al., 2013) have been proposed as parameters to determine the pathways of N_2O production in soils.

Techniques such as acetylene blockage (Balderston et al., 1976; Lin et al., 2019), artificial isotope tracers (^{15}N and ^{18}O) (Mulvaney and Kurtz, 1982; Wrage et al., 2004), and natural stable isotopes (Toyoda et al., 2013; Yu et al., 2020) are conventionally used to identify the pathways of N_2O production via nitrification and denitrification. Both acetylene blockage

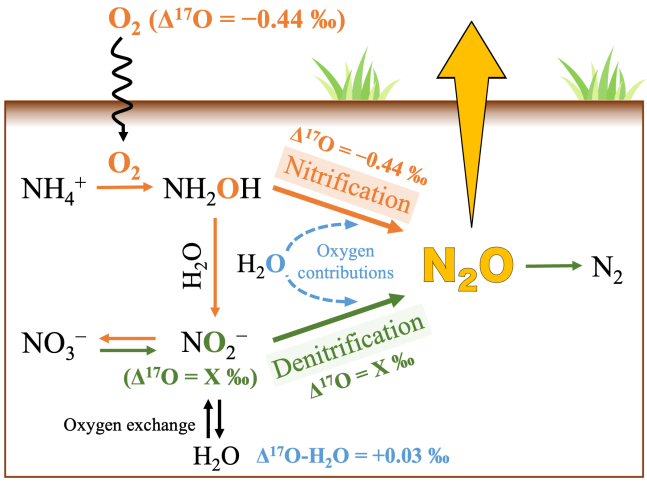

Figure 1. Schematic showing the pathways of N_2O production in soil (Kool et al., 2007, 2011; Wankel et al., 2017; Wrage et al., 2005) and the $\Delta^{17}O$ values of O_2 (Sharp et al., 2016), NO_2^-, and H_2O (Uechi and Uemura, 2019). The orange lines, green lines, and blue dash lines indicate the processes of nitrification, denitrification, and the possible contributions of O atoms derived from soil H_2O through nitrification and denitrification, respectively.

and artificial isotope tracers are mostly performed in laboratory (*in vitro*) incubations because they are costly, complicated, and time-consuming in field research. Natural stable isotopes such as $\delta^{15}N$, $\delta^{18}O$, and SP (^{15}N site preference) can be used to identify the pathways of N_2O production in soils (Decock and Six, 2013; Toyoda et al., 2017; Verhoeven et al., 2019). However, further reduction of N_2O to N_2 after the production of N_2O until emission from soil to air results in significant changes in the $\delta^{15}N$, $\delta^{18}O$, and SP values of N_2O due to the fractionation of isotopes, which makes the identification process difficult (Ostrom et al., 2007).

Recent studies on the $\Delta^{17}O$ value of NO_3^- (the definition detailed in Sect. 2.4) have reported that $\Delta^{17}O$ is a useful natural signature for clarifying the complicated biogeochemical processes in terrestrial ecosystems (Ding et al., 2022, 2023, 2024; Michalski et al., 2004; Tsunogai et al., 2010). Although the values of $\delta^{15}N$, $\delta^{18}O$, and SP can vary during various fractionation processes of isotopes within terrestrial ecosystems, the $\Delta^{17}O$ value remains almost stable because possible variations in $\delta^{17}O$ and $\delta^{18}O$ values during the processes of biogeochemical isotope fractionation follow the relation of $\delta^{17}O \approx 0.5\ \delta^{18}O$, which cancels out the variations in the $\Delta^{17}O$ value (Young et al., 2002). Consequently, the mixing of the same oxygen compounds with different $\Delta^{17}O$ values is the primary cause of variations in $\Delta^{17}O$ values throughout the biogeochemical processes in terrestrial ecosystems.

Because N_2O produced through nitrification is a byproduct of the oxidation reaction between NH_4^+ (to NH_2OH) and O_2, the $\Delta^{17}O$ value of N_2O produced through nitrification is expected to be close to that of tropospheric O_2 (Fig. 1) (Kool et al., 2007, 2011; Wrage et al., 2005), with previous studies reporting a $\Delta^{17}O$ value of −0.44 ‰ (Sharp and Wostbrock, 2021). Conversely, the $\Delta^{17}O$ value of N_2O produced through denitrification is expected to be close to that of NO_2^- (Fig. 1) (Kool et al., 2007, 2011; Wankel et al., 2017; Wrage et al., 2005). Because O atoms in NO_2^- are derived from either soil NO_3^- ($\Delta^{17}O$ = from 0 ‰ to +20 ‰) or H_2O ($\Delta^{17}O = +0.03 \pm 0.01$ ‰) (Hattori et al., 2019; Nakagawa et al., 2018; Uechi and Uemura, 2019), significant differences in $\Delta^{17}O$ values between N_2O produced through nitrification and that produced through denitrification are expected if the additional contributions of O atoms derived from soil H_2O are insignificant in N_2O during the processes of N_2O production in soils through nitrification and denitrification (Fig. 1) (Kool et al., 2007).

Previous studies have identified the elevated $\Delta^{17}O$ values in atmospheric N_2O ($\Delta^{17}O \approx +0.9$ ‰), observed in both stratospheric and tropospheric air (Cliff et al., 1999; Kaiser et al., 2003; Thiemens and Trogler, 1991). Komatsu et al. (2008) subsequently conducted the first $\Delta^{17}O$ measurements of N_2O emitted from a soil to assess whether soil N_2O could be the source of elevated $\Delta^{17}O$ values of atmospheric N_2O. However, the temporal variations of the $\Delta^{17}O$ values for N_2O emitted from soil remain unknown. Whether $\Delta^{17}O$ values of N_2O can be used to identify the pathways of N_2O production in soils has not been discussed. In addition, the advantages of $\Delta^{17}O$ signature, relative to other natural stable isotopes, for identifying the pathways of N_2O production remain unclear. To address these, in this study, we measured precise $\Delta^{17}O$ values for N_2O emitted from forested soil and those for NO_2^- in the soil. Further, we conducted similar observations in the same soil artificially fertilized with Chile saltpeter or urea to investigate the possible contributions of O atoms derived from soil H_2O in N_2O during N_2O production.

2 Methods

2.1 Study site

The study site was located in a secondary warm-temperate forest within an urban area (35°10′ N, 136°58′ E, Fig. 2), approximately 50 m from the common building of the Graduate School of Environmental Studies at Nagoya University. The lowest, highest, and mean monthly temperatures recorded at the nearest meteorological station (Nagoya station) were 5.2 °C (in January), 28.9 °C (in July), and 18.5 °C, respectively, from April 2022 to July 2023. The annual mean precipitation was approximately 1800 mm. The soil stratum in the forested field possessed an approximate depth of 20 cm, characterized by a bulk density of 1.12 g cm^{-3}. Details of the forest have been described in the previous study (Hiyama et al., 2005).

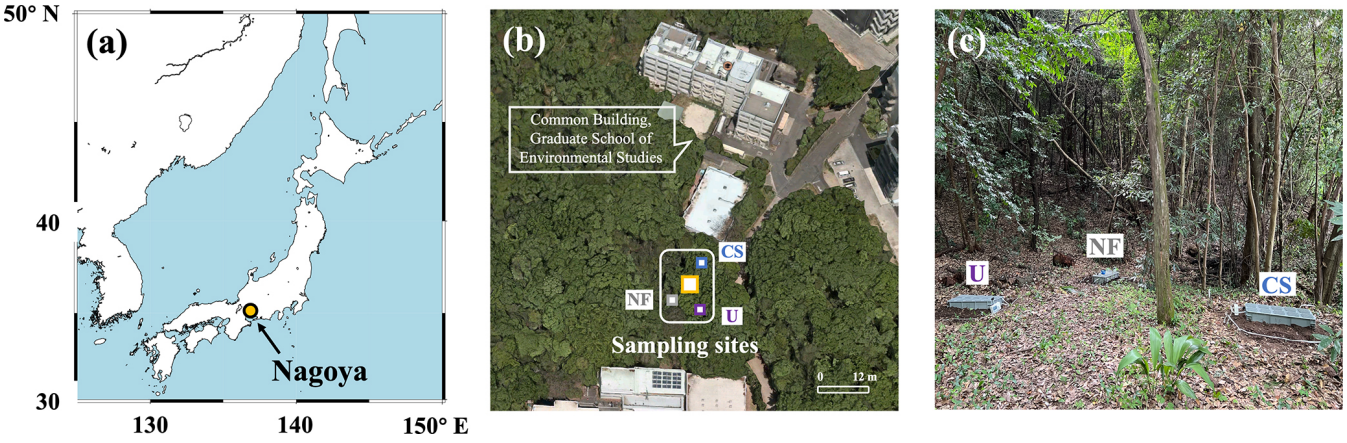

Figure 2. Map showing the location of Nagoya, Japan, where the studied site is located **(a)**. Map showing the monitoring site of N_2O emitted from forested soil in a secondary warm-temperate forest (yellow square) and the plots fertilized with Chile saltpeter (CS, blue square), urea (U, purple square), and no fertilizer (NF, gray square) **(b)**. Photo showing the plots and flow chambers set on the plots **(c)**.

2.2 Sampling of N_2O

Samples of N_2O emitted from the forested soil under natural conditions were collected 18 times ($n = 18$) from April 2022 to July 2023 in a field with an area of 5 m^2 (Fig. 2b). Among the samples, 12 were collected on fine days, whereas 6 were collected on rainy days. A fine day is defined as a day without precipitation for 48 h prior to the end of each sampling. The total precipitation within 12 h at the end of each sampling of the rainy days exceeded 12 mm.

The sampling of N_2O emitted from the artificially fertilized soil was performed during a period of fine weather in three plots (1 m^2 for each located more than 5 m away from each other) within the same forested field, located approximately 3 m away from the plot where we conducted the sampling under natural conditions (Fig. 2b and c). Either urea ($CO(NH_2)_2$, 46 % TN) or Chile saltpeter (KNO_3, 14 % TN) was applied to two of the plots (U and CS plots) on 16 July 2023 at the same N amount of 250 kg N ha^{-1}. Urea is a synthetic N fertilizer (Sun and Hope Ltd., Japan), and Chile saltpeter (SQM Ltd., USA) contains NO_3^- with a high $\Delta^{17}O$ value of +19 ‰ (determined through the internationally distributed isotope reference materials USGS-34 and USGS-35). The third plot was blank, meaning no fertilizer was added (NF plot). Sampling of N_2O from each plot was performed twice on days 2 and 6 after the addition of each fertilizer.

To precisely determine $\Delta^{17}O$ of N_2O, more than 60 nmol of N_2O is required (Komatsu et al., 2008), which corresponds to more than 4 L of air containing N_2O at atmospheric concentrations. Accordingly, in this study, a flow chamber made of polypropylene with dimensions of 0.8 m × 0.3 m × 0.18 m was deployed onto the sampling site throughout each day of sampling (Fig. S1). This chamber has an inlet and outlet port with an inner diameter of 1 cm. The outlet port was connected to an air pump using Tygon tubing, and the inlet port was open to ambient air. Using the air pump, the air in the chamber was taken into a 5 L aluminum bag, along with the gases emitted by the soil, as illustrated in Fig. S1. The flow rate of the air pump was set at 100 mL min^{-1} throughout the deployment of the chamber; thus, each sampling lasted 45 min until 4.5 L of gas was collected into the aluminum bag. Each gas sampling was started 2 h after deployment of the flow chamber; thus, it took more than 8 h to collect four samples. In addition to the gas samples emitted from the soil, ambient air in the forest was sampled into two 3 L vacuum stainless steel canisters (SilcoCan, Restek).

2.3 Sampling and analysis of forested soil

After collecting the gas samples to determine N_2O, a soil sample (approximately 150 g) was randomly collected from more than four places beneath the chamber. Approximately 20 g of the soil sample was heated at 80 °C for 48 h to estimate the water content from the weight loss and water-filled pore space (WFPS; the calculation was detailed in Text S1 in the Supplement). Using the remaining soil sample (120 g), NH_4^+, NO_3^-, and NO_2^- in each soil sample were extracted into 120 mL of a 2 M KCl solution, and their concentrations were determined using a high performance microflow analyzer (QuAAtro 39 Autoanalyzer, BLTEC, Osaka, Japan).

2.4 Concentration and isotopic compositions of N_2O

The gas samples collected in aluminum bags or stainless canisters were subsampled into a 100 mL pre-evacuated glass bottle to determine the concentration ($[N_2O]$), $\delta^{15}N$, and $\delta^{18}O$ of N_2O simultaneously. The remaining samples were further subsampled to either 1 or 2 L pre-evacuated glass bottles to determine the $\Delta^{17}O$ of N_2O. The concentration and isotopic compositions ($\delta^{15}N$, $\delta^{18}O$, and $\Delta^{17}O$) of N_2O were determined using a continuous flow isotope ratio mass spec-

trometry (CF-IRMS; Finnigan MAT252, Thermo Fisher Scientific, Waltham, MA, USA) system that consists of an original pre-concentrator system, chemical traps, and gas chromatograph at Nagoya University (Komatsu et al., 2008). The analytical procedures using the CF-IRMS system were the same as those detailed in previous studies (Hirota et al., 2010; Komatsu et al., 2008).

The isotopic ratios of ^{15}N / ^{14}N, ^{17}O / ^{16}O, and ^{18}O / ^{16}O are expressed in the δ notations:

$$\delta^{15}N, \delta^{17}O, \text{ or } \delta^{18}O = R_{sample}/R_{standard} - 1, \quad (1)$$

where R denotes ^{15}N / ^{14}N, ^{17}O / ^{16}O, or ^{18}O / ^{16}O ratios of the sample and each standard reference material.

The $\Delta^{17}O$ of N_2O, including NO_2^-, NO_3^-, H_2O, and O_2, is defined by Eq. (2) (Kaiser et al., 2007; Miller, 2002):

$$\Delta^{17}O = \frac{1 + \delta^{17}O}{\left(1 + \delta^{18}O\right)^{\beta}} - 1, \quad (2)$$

where β denotes the slope of the reference line in the $\delta^{17}O$–$\delta^{18}O$ space. Previous studies have proposed values ranging from 0.525 to 0.5305 for β during the various processes of isotope fractionation through experimental measurements and/or theoretical calculations (Cao and Liu, 2011; Matsuhisa et al., 1978; Pack and Herwartz, 2014; Sharp and Wostbrock, 2021). In this study, we adopted a value of 0.528 for β to define $\Delta^{17}O$. The details of the ranges of the possible $\Delta^{17}O$ variations due to the ranges of β are presented in Sect. 4.1.

To calibrate the $\delta^{15}N$ and $\delta^{18}O$ of N_2O to the international scale, N_2O in a tropospheric air sample collected at Hateruma Island in 2010 (Japan) was used as the standard with a $\delta^{15}N$ value of +6.5 ‰ and a $\delta^{18}O$ value of +44.3 ‰ (Toyoda et al., 2013). To calibrate the $\Delta^{17}O$ of N_2O on the international Vienna Standard Mean Ocean Water (VSMOW) scale, we prepared two kinds of N_2O standards with different $\Delta^{17}O$ values calibrated using a conventional method (Thiemens and Trogler, 1991). The procedures for this calibration are presented in Sect. 2.6, with the details of the N_2O standards. Through repeated measurements of N_2O in a tropospheric air sample collected at Nagoya University, the analytical precisions (1σ) of the measurements were estimated to be ± 10.0 ppb, ± 0.5 ‰, ± 0.6 ‰, and ± 0.11 ‰ for concentration, $\delta^{15}N$, $\delta^{18}O$, and $\Delta^{17}O$, respectively (Fig. S2). To achieve higher precision, analyses of $\Delta^{17}O$ were performed at least three times for each sample, resulting in a standard error (SE) of ± 0.06 ‰.

2.5 Emission flux

Based on the change in the concentration of N_2O from the inlet to the outlet, the emission flux of N_2O from the soil was calculated using Eq. (3):

$$\text{Flux} = \frac{P \times V \times (C_{final} - C_{air}) \times M}{R \times T \times t \times A}, \quad (3)$$

where Flux denotes the emission flux of N_2O (μg N m^{-2} h^{-1}), P denotes the pressure (Pa), V represents the volume of the gas sample in the aluminum bag (0.0045 m^3), C_{final} denotes the concentration of N_2O in the gas sample taken at the end of each deployment of the chamber (μmol mol^{-1}), C_{air} denotes the concentration of N_2O in the ambient air (μmol mol^{-1}), M represents the molecular weight of N in N_2O (28 μg N μmol^{-1}), R represents the universal gas constant (8.314 m^3 Pa K^{-1} mol^{-1}), T represents the air temperature in the forest (K), t represents the duration of each gas sampling (45 min), and A represents the surface area of soil covered by the chamber (0.24 m^2).

2.6 Calibration of the $\Delta^{17}O$ values of N_2O

To determine the $\Delta^{17}O$ values of N_2O in the samples on the VSMOW scale, we prepared two standards (STD1 and STD2) containing N_2O. The $\Delta^{17}O$ values of N_2O in the standards were calibrated to the VSMOW scale using the conventional method reported in Thiemens and Trogler (1991), where N_2O was quantitatively converted to O_2 using BrF_5 and a Ni catalytic container. The details are presented below.

A calibrated quantity of N_2O (50–170 μmol) was subsampled and transferred into a nickel tube (approximately 60 cm^3) under liquid N_2 temperature. The coexisting components of N_2O, such as helium in the case of STD2, were evacuated from the nickel tube after N_2O was trapped in the nickel tube under liquid N_2 temperature. The nickel tube was then heated at 725 °C for 2.5 h to convert N_2O to NiO and N_2. After evacuating N_2 from the nickel tube, a 10-fold quantity of BrF_5 was introduced into the nickel tube and heated at 725 °C for 12 h to convert NiO to O_2 and NiF_2. After the purification of O_2, both $\delta^{18}O$ and $\Delta^{17}O$ of O_2 were determined on the VSMOW scale using IRMS, with the quantity of O_2 evolved from N_2O. Details on the procedures of O_2 purification and the measurement of O_2 using IRMS on the VSMOW scale have been described in previous studies (Sambuichi et al., 2021, 2023). STD1 is pure N_2O gas prepared from N_2O in a gas cylinder (more than 99.9 %; Koike Medical Ltd., Japan). The yield ratios of O_2 and $\Delta^{17}O$ of STD1 were 103 ± 7 % and −0.22 ± 0.07 ‰, respectively (Fig. S3). The N_2O in STD2 is a mixture of helium and N_2O (N_2O / He ≈ 1.5) produced from NO_2^- that had been under oxygen isotope exchange equilibrium with H_2O with a $\Delta^{17}O$ value of +1.2 ‰ originally, under a pH of 1.2. NO_2^- was then converted to N_2O through a reaction with hydrazoic acid (N_3H), as described by Tsunogai et al. (2008). The reaction product (N_2O) was purged from the vial using pure helium (more than 99.9 %). After the removal of H_2O by passing a trap under the temperature of dry ice + ethanol, N_2O was captured in a trap at the temperature of liquid O_2 and then transported into a 1 L stainless steel canister together with helium. The yield of O_2 and $\Delta^{17}O$ of STD2 were 97 ± 5 % and +1.13 ± 0.02 ‰, respectively (Fig. S3). To calibrate the

$\Delta^{17}O$ values of the samples measured using CF-IRMS, approximately 1 mL of each STD was subsampled into a 200-mL pre-evacuated glass bottle and diluted using pure helium to 1 atm. The $\Delta^{17}O$ values of N_2O in the diluted standards were then determined using CF-IRMS like the procedure used on the samples before the sample measurements by introducing 30–60 nmol of N_2O. This allowed us to calibrate the $\Delta^{17}O$ values of the samples to the VSMOW scale (Fig. S4).

2.7 Isotopic composition of NO_2^-

To determine the $\delta^{18}O$ and $\Delta^{17}O$ values of soil NO_2^- that had been extracted in the KCl solution, the NO_2^- in the KCl solution was chemically converted to N_2O using the method originally developed to determine the $\delta^{18}O$ of NO_2^- (McIlvin and Altabet, 2005), with several modifications for $\Delta^{17}O$ (Xu et al., 2021), as explained below. Approximately 40 mL of each solution was pipetted into a glass vial (66.7 mL) and sealed with a butyl rubber septum cap. After purging the solution using high-purity helium for 45 min, 1.8 mL of an azide-acetic acid buffer (0.1 mol L^{-1} NaN_3 in 1 vol % acetic acid), which had been purged using pure helium as well, was added to the solution to convert NO_2^- to N_2O:

$$HNO_2 + HN_3 \rightarrow N_2O + H_2O + N_2. \quad \text{(R1)}$$

After the vials were shaken for 1 h at a rate of 2 cycles s^{-1}, 0.9 mL of 6 M NaOH was added to each vial and shaken for 15 min.

The $\delta^{18}O$ and $\Delta^{17}O$ of N_2O converted from NO_2^- in each vial were determined using the CF-IRMS system. We repeated the analyses for each solution sample at least three times to obtain better precision for $\Delta^{17}O$.

The $\delta^{18}O$ values of NO_2^- were calibrated to the VSMOW scale using three in-house nitrite standards (STD10, STD11, and STD12), the $\delta^{18}O$ values of which had been determined using a thermal conversion elemental analyzer IRMS system, where oxygen atoms in each nitrite / nitrate had been converted into CO using a glassy carbon tube at 1400 °C (Xu et al., 2021) and calibrated to the VSMOW scale using the international nitrate standards USGS34 ($\delta^{18}O = -27.9$ ‰) and IAEA-NO-3 ($\delta^{18}O = +25.6$ ‰) as the primary standards. Isotope fractionations during chemical conversion into N_2O were corrected by measuring the nitrite standards in the same way as samples were measured using the CF-IRMS system. In addition, the extent of oxygen isotope exchange between NO_2^- and H_2O during the conversion was quantified using the relation between $\delta^{18}O$ of the nitrite standards and that of N_2O (Xu et al., 2021). The $\Delta^{17}O$ values of NO_2^- were calibrated to the VSMOW scale by comparing N_2O derived from NO_2^- with N_2O standards (STD1 and STD2) while assuming that the changes in $\Delta^{17}O$ were negligible during the conversion from NO_2^- into N_2O, except for the oxygen isotope exchange reaction between NO_2^- and H_2O during the conversion to N_2O. The progress of oxygen isotope exchange between NO_2^- and H_2O was calibrated from the $\Delta^{17}O$ values of NO_2^- using the exchange rate estimated by calculating $\delta^{18}O$ values while assuming that the $\Delta^{17}O$ value of H_2O was 0 ‰.

While the KCl solutions were widely used for the extraction of soil NO_2^- (e.g., Lewicka-Szczebak et al., 2021; Shen et al., 2003), Homyak et al. (2015) raised the concerns that the recovery of soil NO_2^- could be low when using KCl solutions compared to deionized water. Therefore, we conducted a comparative experiment to evaluate this potential issue and concluded that the use of KCl solution introduced negligible bias in terms of soil NO_2^- recovery or $\Delta^{17}O$ measurements compared to deionized water extraction for the soil type and experimental conditions in this study. The details are described in the Supplement (Text S2).

3 Results

3.1 Flux and isotopic compositions of N_2O emitted from forested soil

Almost all of the concentrations of N_2O ($[N_2O]$) in the samples collected in aluminum bags were higher than that of N_2O in ambient air (Figs. 3a and S5), implying that N_2O in the aluminum bags was a mixture of N_2O in ambient air and N_2O emitted from the forested soil. To determine the isotopic compositions ($\delta^{15}N$, $\delta^{18}O$, and $\Delta^{17}O$) of N_2O emitted from the soil, N_2O derived from ambient air was excluded using the linear correlation between $1/[N_2O]$ and the isotopic compositions ($\delta^{15}N$, $\delta^{18}O$, and $\Delta^{17}O$) during mixing (Figs. 3b, c, d, and S5), also was known as Keeling plot approach (Keeling, 1958; Tsunogai et al., 1998, 2003). This method assumes that the concentrations of N_2O ($N_2O / (N_2O + N_2)$) in the gases emitted from the soil were more than 3 %, allowing $1/[N_2O]$ to be approximated to be 0 (Text S3). The uncertainties associated with the isotopic compositions of N_2O emitted from soil (i.e., the intercept) were estimated by applying the York method (Tsunogai et al., 2011; York et al., 2004) to the obtained relationship between $1/[N_2O]$ as the independent variable and the isotopic compositions as the dependent variable in which uncertainties of both independent and dependent variables for individual data are considered.

The flux of N_2O emitted from the forested soil determined on fine days varied from −0.2 to 9.8 μg N m^{-2} h^{-1}, with an average of 3.8 ± 3.1 μg N m^{-2} h^{-1} (1 SD; $n = 12$). In addition, the emission flux during the warm seasons (from April to October; 5.1 ± 2.8 μg N m^{-2} h^{-1}) was significantly higher than that during the cold seasons (from November to March; 1.0 ± 1.1 μg N m^{-2} h^{-1}) (Fig. 4a; Table S1), implying that the emission flux of N_2O on fine days exhibited clear seasonal variation. Furthermore, the average emission flux of N_2O determined on rainy days (38.8 ± 28.0 μg N m^{-2} h^{-1}; $n = 6$) was significantly higher than that determined on fine

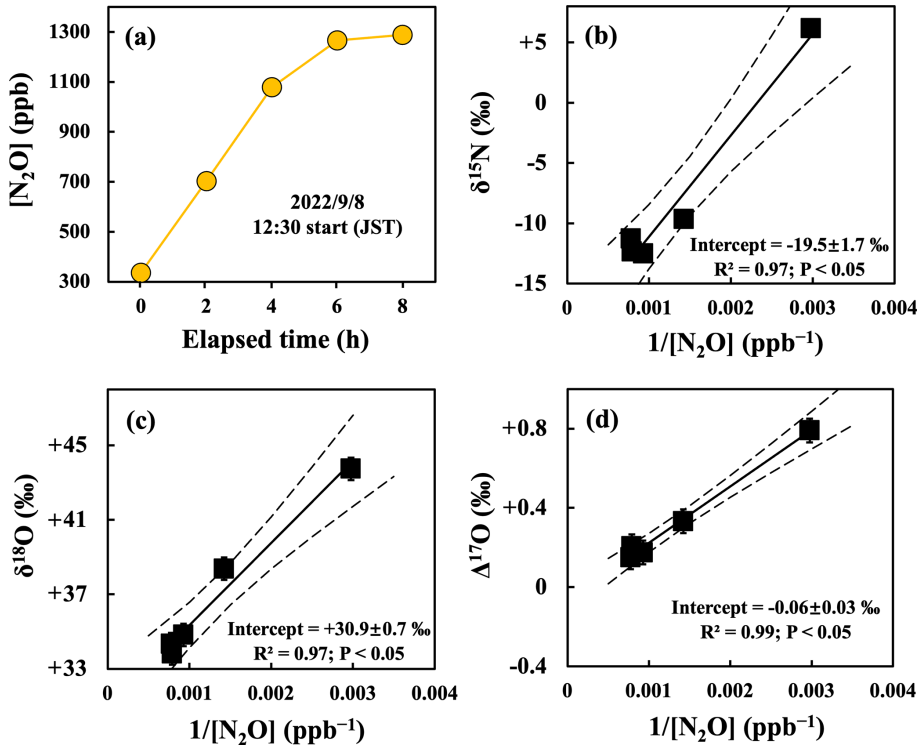

Figure 3. An example of changes in the concentration of N_2O ($[N_2O]$) in gas samples during the observation on 8 September 2022, plotted as a function of the elapsed time since the deployment of the flow chamber on the forested soil **(a)**, and the $\delta^{15}N$ **(b)**, $\delta^{18}O$ **(c)**, and $\Delta^{17}O$ **(d)** values of N_2O plotted as a function of the reciprocal of $[N_2O]$ ($1/[N_2O]$) during the observation. Each solid line is the least squares fitting of the samples, while each dotted line is the 2σ confidence interval of the fitting line. Error bars smaller than the sizes of the symbols are not shown.

days (3.8 ± 3.1 µg N m^{-2} h^{-1}) (Fig. 4a and b). These patterns of N_2O emissions were in accordance with those of agricultural and forested soils reported in previous studies (Anthony et al., 2023; Chen et al., 2012; Choudhary et al., 2002; Yan et al., 2008).

Because of the small emission flux of N_2O during the cold seasons, the linear relationships between the isotopic compositions and $1/[N_2O]$ became insignificant in some of the observations performed during the cold seasons (Fig. S5, from November 2022 to January 2023). Thus, the uncertainties associated with the isotopic compositions estimated for N_2O emitted from the soil became enormous. Consequently, the isotopic compositions of N_2O emitted from the soil are not shown under the following conditions: (1) the $[N_2O]$ in the gas sample collected at the end of each deployment of the chamber did not exceed 130 % of that of ambient air, and (2) the linear correlation between $1/[N_2O]$ and the isotopic compositions was statistically insignificant ($P > 0.05$). Similar criteria have been adopted in previous studies (Kaushal et al., 2022; Opdyke et al., 2009).

The N_2O emitted from the forested soil on fine days exhibited $\delta^{15}N$, $\delta^{18}O$, and $\Delta^{17}O$ values ranging from −27.5 ‰ to −17.9 ‰, from +26.1 ‰ to +37.6 ‰, and from −0.40 ‰ to −0.11 ‰, respectively, with average values and standard deviations (1 SD) of -22.5 ± 2.8 ‰, $+30.9 \pm 4.3$ ‰, and -0.30 ± 0.09 ‰, respectively (Fig. 4g, e, and c). On the other hand, N_2O emitted from the forested soil on rainy days exhibited $\delta^{15}N$, $\delta^{18}O$, and $\Delta^{17}O$ values ranging from −26.6 ‰ to −13.8 ‰, from +18.4 ‰ to +36.2 ‰, and from −0.06 ‰ to +0.26 ‰, respectively, with average values and standard deviations (1SD) of -20.4 ± 5.0 ‰, $+27.9 \pm 6.4$ ‰, and $+0.12 \pm 0.13$ ‰, respectively (Fig. 4g, e, and c).

The NO_2^- exhibited $\delta^{18}O$ and $\Delta^{17}O$ values ranging from +2.4 ‰ to +12.0 ‰ and from +0.04 ‰ to +0.50 ‰, respectively, with average values of $+6.0 \pm 2.0$ ‰ and $+0.23 \pm 0.12$ ‰, respectively ($n = 18$, Fig. 4e and c). These $\delta^{18}O$ values of NO_2^- coincided well with those determined in a previous study (Lewicka-Szczebak et al., 2021).

3.2 Flux and isotopic compositions of N_2O emitted from artificially fertilized soils

The fluxes of N_2O emitted from the NF (no fertilizer), U (fertilized with urea, $CO(NH_2)_2$), and CS (fertilized with Chile saltpeter, KNO_3) plots were 5.2, 70.6, and 112.3 µg N m^{-2} h^{-1}, respectively, 2 d after fertilization and 4.2, 56.7, and 39.4 µg N m^{-2} h^{-1}, respectively, 6 d after fertilization (Table S1). The fluxes of N_2O emitted from the U and CS

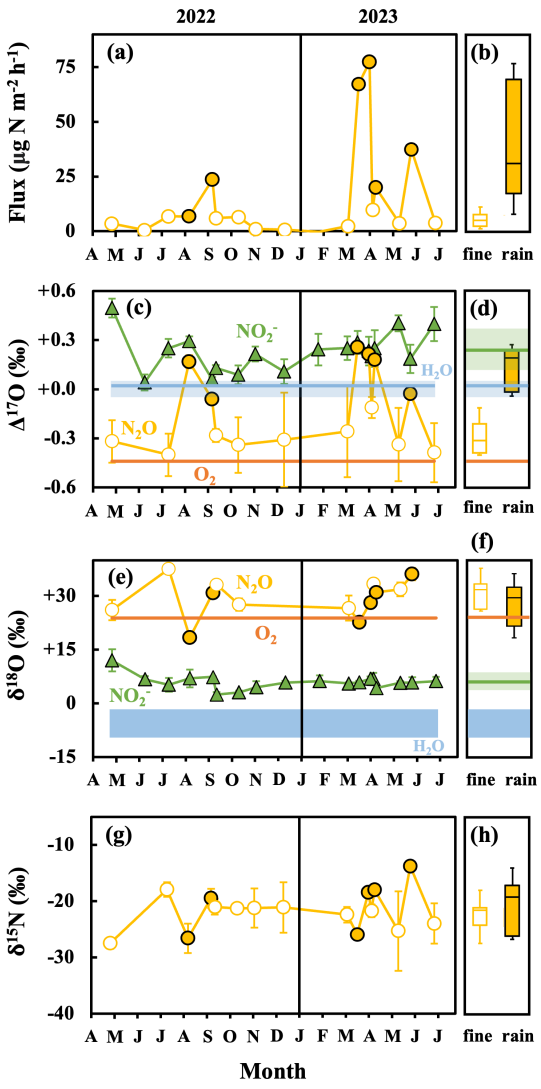

Figure 4. Temporal variations in the flux **(a)**, $\Delta^{17}O$ **(c)**, $\delta^{18}O$ **(e)**, and $\delta^{15}N$ **(g)** values of N_2O emitted from the forested soil, and the $\delta^{18}O$ and $\Delta^{17}O$ values of soil NO_2^- (green triangles), O_2 (orange lines), and soil H_2O (blue area or line). Sampling performed on fine and rainy days is indicated by the open (white) and solid (yellow) circles, respectively, with the box plots of the emission flux **(b)**, $\Delta^{17}O$ **(d)**, $\delta^{18}O$ **(f)**, and $\delta^{15}N$ **(h)** of N_2O on fine and rainy days. The black lines of the box plots indicate the median values. The lower and upper boundaries of the box plots indicate the lower (25 %) and upper (75 %) quartiles of data for each component, respectively. The whiskers of the box plots denote the entire range of values for each component. Error bars smaller than the sizes of the symbols are not shown.

plots were significantly higher than that from the NF plot, indicating that the flux of N_2O emitted from the soil increased significantly because of fertilization, supporting the results reported in previous studies (Kaushal et al., 2022; McKenney et al., 1978; Toyoda et al., 2011, 2017).

The $\delta^{15}N$, $\delta^{18}O$, and $\Delta^{17}O$ values of N_2O emitted from the NF plot 2 d after fertilization were -17.1 ± 6.4 ‰, $+36.1 \pm 6.7$ ‰, and -0.37 ± 0.20 ‰, respectively, whereas those emitted from the NF plot 6 d after fertilization were -12.2 ± 3.2 ‰, $+40.0 \pm 13.3$ ‰, and -0.32 ± 0.23 ‰, respectively. The $\delta^{15}N$, $\delta^{18}O$, and $\Delta^{17}O$ values of N_2O emitted from the U plot 2 d after fertilization were -39.3 ± 0.7 ‰, $+34.4 \pm 0.4$ ‰, and -0.14 ± 0.06 ‰, respectively, whereas those emitted from the U plot 6 d after fertilization were -33.3 ± 0.5 ‰, $+25.7 \pm 0.6$ ‰, and -0.16 ± 0.05 ‰, respectively. The $\delta^{15}N$, $\delta^{18}O$, and $\Delta^{17}O$ values of N_2O emitted from the CS plot 2 d after fertilization were -19.3 ± 0.6 ‰, $+54.1 \pm 0.8$ ‰, and $+8.22 \pm 0.03$ ‰, respectively, whereas those emitted from the CS plot 6 d after fertilization were -11.3 ± 0.7 ‰, $+58.7 \pm 1.2$ ‰, and $+7.36 \pm 0.17$ ‰, respectively (Fig. 5). These flux, $\delta^{15}N$, and $\delta^{18}O$ of N_2O emitted from the NF, U, and CS plots correspond well with the results of many previous studies on forested and artificial soils (or agricultural soils) (Kaushal et al., 2022; Kim and Craig, 1993; Snider et al., 2009; Toyoda et al., 2017; Wrage et al., 2004).

The $\delta^{18}O$ and $\Delta^{17}O$ values of NO_2^- in the NF plot 2 d after fertilization were +2.7 ‰ and +0.42 ‰, respectively, whereas those in the NF plot 6 d after fertilization were +1.3 ‰ and +0.35 ‰, respectively. The $\delta^{18}O$ and $\Delta^{17}O$ values of NO_2^- in the U plot 2 d after fertilization were +7.6 ‰ and +0.31 ‰, respectively, whereas those in the U plot 6 d after fertilization were +5.4 ‰ and +0.17 ‰, respectively. The $\delta^{18}O$ and $\Delta^{17}O$ values of NO_2^- in the CS plot 2 d after fertilization were +29.0 ‰ and +8.26 ‰, respectively, whereas those in the CS plot 6 d after fertilization were +45.2 ‰ and +12.32 ‰, respectively (Fig. 6).

4 Discussion

4.1 Identification of N_2O production pathways in forested soil using $\Delta^{17}O$ signature

Because O atoms in N_2O emitted from soil can be derived from those in NO_2^-, O_2, or H_2O in soil (Fig. 1), we can constrain the pathways of N_2O production by comparing the $\delta^{18}O$ and $\Delta^{17}O$ values of N_2O with those of NO_2^-, O_2, and H_2O in soil. Consequently, we compiled the $\delta^{18}O$ and $\Delta^{17}O$ values of atmospheric O_2 (+23.88 ‰ for $\delta^{18}O$ and −0.44 ‰ for $\Delta^{17}O$, Sharp and Wostbrock, 2021) and rainwater (ranging from −2 ‰ to −10 ‰ for $\delta^{18}O$ in Japan, Nakagawa et al., 2018; Takahashi, 1998; Uechi and Uemura, 2019; Zou et al., 2015; +0.03 ‰ for $\Delta^{17}O$ in Japan, Uechi and Uemura, 2019), as shown in Figs. 4 and 6, along with those of soil NO_2^- measured in this study.

The $\Delta^{17}O$ of N_2O produced in the soil may differ from that of the source of O atoms (O_2, NO_2^-, H_2O) because of oxygen isotope fractionation during nitrification and denitrification, as the value of β in Eq. (2) may vary depending on

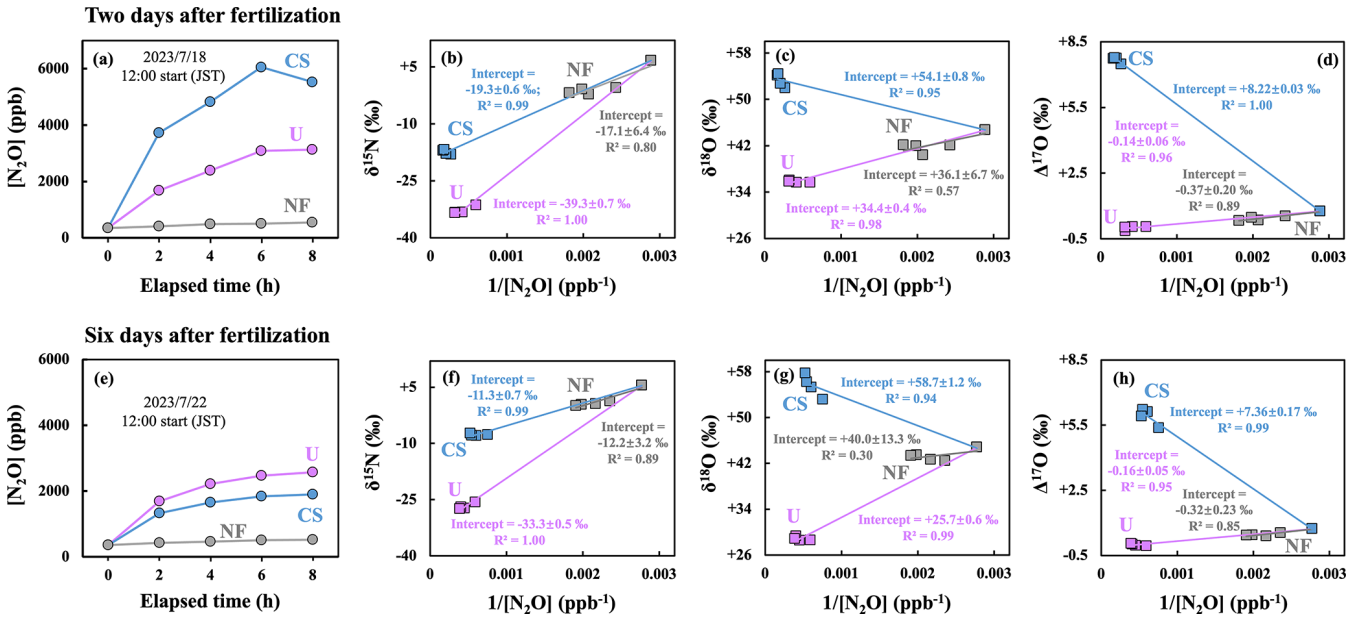

Figure 5. Changes in $[N_2O]$ of gas samples collected from the plots of NF (gray), U (purple), and CS (blue) 2 d after fertilization **(a)** and 6 d after fertilization **(e)** and plotted as a function of the elapsed time since the deployment of the flow chamber; the $\delta^{15}N$ **(b, f)**, $\delta^{18}O$ **(c, g)**, and $\Delta^{17}O$ **(d, h)** values of N_2O plotted as a function of the reciprocal of $[N_2O]$ ($1/[N_2O]$). Error bars smaller than the sizes of the symbols are not shown.

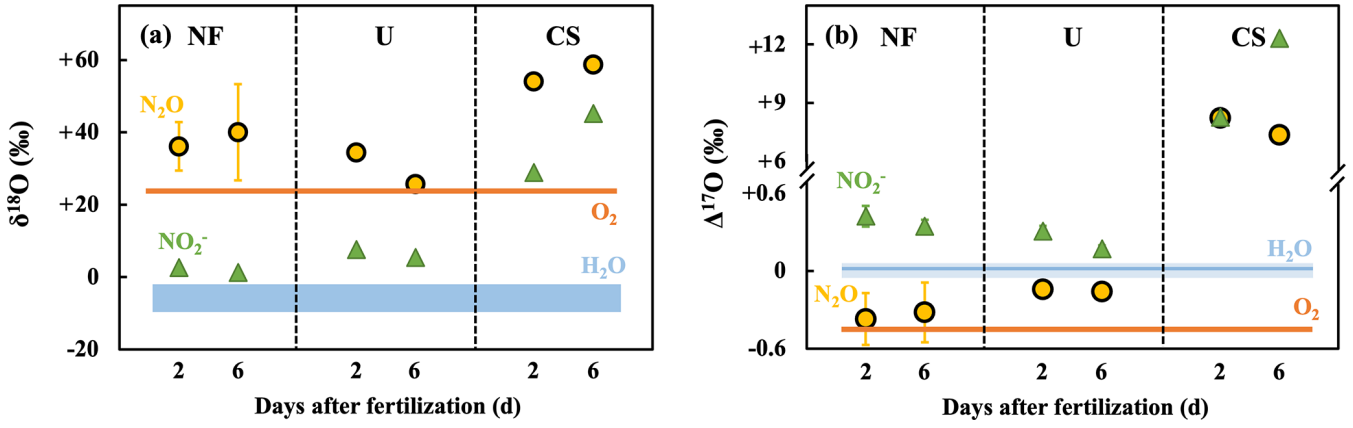

Figure 6. The $\delta^{18}O$ **(a)** and $\Delta^{17}O$ **(b)** values of N_2O (yellow circles) and NO_2^- (green triangles) in NF, U, and CS plots determined 2 and 6 d after fertilization, and the $\delta^{18}O$ and $\Delta^{17}O$ values of O_2 (orange lines) and soil H_2O (blue area or line). Error bars smaller than the sizes of the symbols are not shown.

the reactions. Thus, prior to using $\Delta^{17}O$ values to identify the pathways of N_2O production in soils, we quantified the possible variations in the $\Delta^{17}O$ values of N_2O during each reaction. The details are presented below.

The fractionation of oxygen isotopes during the transformation of the O atoms in O_2 to those in N_2O through nitrification accompanies significant variations in the value of $\delta^{18}O$ from O_2 to N_2O (Figs. 4e and 6a). In addition to $\delta^{18}O$, the $\Delta^{17}O$ value of N_2O produced through nitrification could be somewhat different from that of O_2, even if all O atoms in N_2O were derived from O_2, due to the possible differences in β from 0.528 during the reaction (Fig. 7). The average variation in $\delta^{18}O$ from O_2 to N_2O due to nitrification ($\Delta\delta^{18}O$ (N_2O-O_2)) was estimated to be 9 ‰ on average (Figs. 4e and 6a) based on the difference in $\delta^{18}O$ values between N_2O emitted from the soil in this study ($+33 \pm 10$ ‰; $n = 19$) and O_2 in the literature (Sharp and Wostbrock, 2021). Conversely, we can expect values from 0.525 to 0.5305 for β in the various reactions (Cao and Liu, 2011; Matsuhisa et al., 1978; Pack and Herwartz, 2014; Sharp and Wostbrock, 2021), where the β of nitrification may be included. Thus, we quantified the possible range of variations in the $\Delta^{17}O$ value

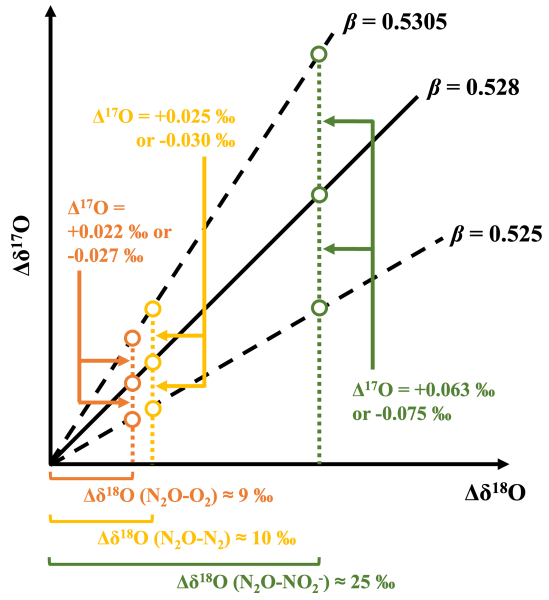

Figure 7. Schematic showing the possible variations in the $\Delta^{17}O$ value of N_2O from that of the source of O atoms (O_2 and NO_2^-) during transformations, including nitrification (orange circles), denitrification (green circles), and reduction (yellow circles), due to variations in isotope fractionation and β from 0.525 to 0.5305.

of N_2O from that of O_2 to be less than 0.027 ‰ (Fig. 7), based on the observed $\Delta\delta^{18}O(N_2O-O_2)$ and the possible variation range of β.

Similarly, the fractionation of oxygen isotopes during the transformation of O atoms in NO_2^- to those in N_2O through denitrification accompanies significant variations in $\delta^{18}O$ from NO_2^- to N_2O as well. The $\Delta^{17}O$ value of N_2O produced through NO_2^- reduction could be somewhat different from that of NO_2^-, even if all O atoms in N_2O were derived from NO_2^-, due to the possible differences in β from 0.528 during the reaction (Fig. 7). The average variation in $\delta^{18}O$ from NO_2^- to N_2O due to fractionation ($\Delta\delta^{18}O$ ($N_2O-NO_2^-$)) was estimated to be 25 ‰ on average (Figs. 4e and 6a) based on the difference in $\delta^{18}O$ values between N_2O ($+33 \pm 10$ ‰; $n = 19$) and NO_2^- in this study ($+8 \pm 9$ ‰; $n = 24$). Thus, we quantified the possible range of variations in the $\Delta^{17}O$ value of N_2O from that of NO_2^- to be less than 0.075 ‰ (Fig. 7), based on the observed $\Delta\delta^{18}O$ (N_2O–NO_2^-) and the possible variation range of β, from 0.525 to 0.5305.

Similarly, kinetic fractionation during the reduction of N_2O to N_2 accompanies variation in $\delta^{18}O$ from original N_2O to residual N_2O as well. The $\Delta^{17}O$ value of residual N_2O could somewhat differ from that of the original N_2O. Previous studies have reported the range of variations in $\delta^{18}O$ from original N_2O to residual N_2O due to kinetic fractionation to be less than 10 ‰ on average through incubation experiments (Lewicka-Szczebak et al., 2014, 2015). Thus, we quantified the possible range of variations in the $\Delta^{17}O$ value of residual N_2O from that of original N_2O to be less than 0.03 ‰ (Fig. 7), based on $\Delta\delta^{18}O$ (less than 10 ‰) and the variation range of β, from 0.525 to 0.5305.

These possible variations in $\Delta^{17}O$ (less than 0.075 ‰) were much less than the difference in $\Delta^{17}O$ values between O_2 and NO_2^- in the forested soil (0.7 ‰ on average; Fig. 4c). In addition, the possible variation ranges in $\Delta^{17}O$ become much smaller if the differences in β from 0.528 were smaller than those used in the calculations (from 0.525 to 0.5305). Thus, we concluded that the possible variations in the $\Delta^{17}O$ value of N_2O from that of the source molecules of O atoms (O_2, H_2O, and NO_2^-) during the transformations, including nitrification, denitrification, and reduction, were negligible.

While the $\Delta^{17}O$ values of soil O_2 and H_2O used in this study were referred from atmospheric O_2 and rainwater, respectively, the processes in soil, including diffusion and respiration of O_2 and evaporation and infiltration of rainwater, may cause significant isotopic fractionations of $\delta^{18}O$, which could consequently alter the $\Delta^{17}O$ values of atmospheric O_2 and rainwater. Thus, prior to using $\Delta^{17}O$ values to identify the pathways of N_2O production in soils, we evaluated the possible variations in the $\Delta^{17}O$ values of O_2 and H_2O in soil compared to those of atmospheric O_2 and rainwater. The details are presented below.

For soil O_2, Aggarwal and Dillon (1998) measured the $\delta^{18}O$ values in soil gas at a depth of 3–4 m at a site near Lincoln, Nebraska, USA ranged from +23.3 ‰ to +27.2 ‰, showing the values were comparable with that of atmospheric O_2 (+23.5 ‰ after adjustment in Aggarwal and Dillon, 1998). This confirms that the isotopic fractionations of soil O_2 induced from soil respiration and diffusion processes were not significant. Because the maximum variation in $\delta^{18}O$ from atmospheric O_2 to soil O_2 was less than 3.7 ‰ (27.2 ‰–23.5 ‰), using the method presented in Fig. 7, we quantified the possible variations in the $\Delta^{17}O$ value of soil O_2 from that of atmospheric O_2 to be less than 0.01 ‰. Thus, we ignored the negligible variations in this study.

Similarly, for soil H_2O, Lyu (2021) observed that $\delta^{18}O$ values in soil H_2O at the depths of 0–5, 15–20, and 40–45 cm in a subtropical forest plantation ranged from −4 ‰ to −10 ‰, which fully overlapped with local rainwater (−1 ‰ to −16 ‰), indicating insignificant isotopic fractionations of soil H_2O during hydrological processes such as infiltration and evaporation. In addition, Aron et al. (2021) compiled $\Delta^{17}O$ values of terrestrial H_2O including rainwater, surface, and subsurface water in earth, ranging from +0.06 ‰ to −0.06 ‰ which did not show significant differences with each other, also indicating that the possible variations of $\Delta^{17}O$ values of soil H_2O compared to that of rainwater should be negligible. Finally, we added the variations of $\Delta^{17}O$ values (+0.06 ‰ to −0.06 ‰) of terrestrial H_2O reported in Aron et al. (2021) to Figs. 4 and 6 as the uncertainties of $\Delta^{17}O$ values of soil H_2O.

In the forested soil, N_2O exhibited $\Delta^{17}O$ values (-0.30 ± 0.09 ‰ on average) that were close to that of O_2 (−0.44 ‰) but deviated from those of soil NO_2^- on fine

days ($+0.24 \pm 0.14$ ‰; Fig. 4c and d), implying that nitrification was the main pathway to produce N_2O in the soil on fine days. Conversely, N_2O emitted from the soil on rainy days exhibited $\Delta^{17}O$ values ($+0.12 \pm 0.13$ ‰) that were close to those of soil NO_2^- ($+0.22 \pm 0.09$ ‰) and soil H_2O ($+0.03$ ‰) but deviated from that of O_2 (Fig. 4c and d), implying that (1) the main pathway to produce N_2O changed from nitrification on fine days to denitrification on rainy days and/or (2) the possible contribution of O atoms derived from soil H_2O became more active during the production of N_2O in the soil on rainy days.

4.2 Changes in the $\Delta^{17}O$ of N_2O emitted from artificially fertilized soils

To quantitatively constrain the possible contributions of O atoms derived from soil H_2O during the production of N_2O in the soil, we observed changes in the isotopic compositions of N_2O from the same soil in response to artificial fertilization. In the plot fertilized with CS, the $\Delta^{17}O$ value of N_2O emitted from the soil ($+7.79 \pm 0.61$ ‰ on the average of 2 and 6 d after the fertilization) became significantly closer to that of soil NO_2^- ($+10.3 \pm 2.9$ ‰) compared with that of atmospheric O_2 (-0.44 ‰; Fig. 6b). This suggested that denitrification became the main pathway of N_2O production, probably because of fertilization, which resulted in a significantly higher concentration of NO_3^- (278.4 ± 43.2 mg N kg^{-1}; Table S1) than that of NH_4^+ (15.8 ± 4.1 mg N kg^{-1}) in the CS plot. In addition, N_2O emitted from the CS plot exhibited $\Delta^{17}O$ values that were significantly different from those of soil H_2O ($+0.03$ ‰; Fig. 6b), implying that the contribution of O atoms derived from soil H_2O was minor during the reduction of NO_2^- to produce N_2O. If all the O atoms with low $\Delta^{17}O$ values in N_2O were derived from soil H_2O ($+0.03$ ‰) in the CS plot, the contribution of O atoms derived from soil H_2O was calculated to be 24 % ((10.30 ‰–7.79 ‰) / (10.30 ‰–0.03 ‰)), based on the isotopic mass balance. If the O_2 also contributed to the N_2O production in the CS plot, the contribution of O atoms derived from soil H_2O should be further reduced. As a result, we determined that the maximum possible contribution of O atoms derived from soil H_2O during the reduction of NO_2^- to N_2O was 24 %.

On the other hand, in the plot fertilized with urea (U plot), the $\Delta^{17}O$ value of N_2O (-0.15 ± 0.01 ‰) was close to that of O_2 (-0.44 ‰) compared with that of soil NO_2^- ($+0.24 \pm 0.10$ ‰). This suggested that nitrification was the main pathway of N_2O production (Fig. 6b), probably due to the enhancement of NH_4^+ concentration (423.1 ± 18.2 mg N kg^{-1}; Table S1) compared with that of NO_3^- (13.0 ± 10.7 mg N kg^{-1}) in the U plot. In addition, N_2O emitted from the U plot exhibited $\Delta^{17}O$ values that were significantly different from that of soil H_2O ($+0.03$ ‰; Fig. 6b), implying that the contribution of O atoms derived from soil H_2O was also minor during the oxidation of NH_4^+ to produce N_2O. Consequently, the contribution of O atoms derived from soil H_2O was minor in the soil during N_2O production, irrespective of the pathways of N_2O production being either nitrification or denitrification. In addition, it is difficult to explain the observed increases in the emission flux of N_2O from the soil on rainy days based only on the active contribution of O atoms derived from soil H_2O. Consequently, we concluded that N_2O production through denitrification became active in the soil on rainy days, which resulted in increased N_2O emission and higher $\Delta^{17}O$ values.

4.3 Verification of active N_2O emission by denitrification on rainy days

The forested soil exhibited significantly lower WFPS on fine days (66.1 ± 6.2 %; Table S1) than on rainy days (95.6 ± 19.1 %), implying that the O_2 concentration in the soil was higher on fine days than on rainy days. Using the isotope tracer enriched in ^{15}N ($^{15}NO_3^-$ or $^{15}NH_4^+$), Mathieu et al. (2006) estimated the relative importance of nitrification and denitrification to produce N_2O in soil. They found that nitrification produced the majority of N_2O under low WFPS conditions (75 %), whereas denitrification accounted for more than 85 % of N_2O produced under high WFPS conditions (150 %). Similarly, using natural stable isotopes (SP), Ibraim et al. (2019) reported the primary pathway for N_2O production in a grassland shifted from nitrification to denitrification as increasing WFPS, when WFPS was below 90 %. Thus, we conclude that the lower WFPS in the soil caused oxic conditions on fine days, resulting in nitrification as the primary pathway for N_2O production in the soil. Conversely, the higher WFPS caused redox conditions in the soil on rainy days, resulting in active N_2O production through denitrification in the soil (Fig. 4a and b).

During continuous monitoring of the emission flux of N_2O from an agricultural soil for four years, Anthony et al. (2023) found short-term increases in the emission flux during or immediately after rainfall or irrigation. They referred to this high emission flux as "hot moments" and defined it as exceeding four standard deviations of that of normal periods. They also found significant correlations between the emission flux and WFPS, leading to the conclusion that variations in the concentrations of O_2 in surface soils were responsible for the hot moments of N_2O emissions. Although the hot moments accounted for 1 % of all measurements, they contributed up to 57 % of the annual emissions, indicating their significance as a source of atmospheric emissions. In this study, the emission flux of N_2O on rainy days also exceeded four standard deviations of that on fine days (Fig. 4a and b). The $\Delta^{17}O$ evidence of N_2O found in this study further verified that denitrification was mainly responsible for the enhancement of N_2O production during the hot moments.

4.4 Changes in the pathway of N_2O production due to fertilization with urea

During our observation on the plot fertilized with urea (U plot), N_2O emitted from the plot exhibited $\Delta^{17}O$ values (-0.15 ± 0.01 ‰ on average; Fig. 6b) that were significantly higher than those of the plot without fertilization (NF plot; -0.35 ± 0.04 ‰ on average). Although an increase in the contribution of O atoms derived from soil H_2O could be responsible for the $\Delta^{17}O$ values in addition to an increase in N_2O production through nitrification, we concluded that an increase in N_2O production through NO_2^- reduction was responsible for the $\Delta^{17}O$ values (-0.15 ± 0.01 ‰ on average) of N_2O produced in the plot in response to fertilization of urea / NH_4^+ for the following reasons.

Avrahami et al. (2002) reported that fertilization with urea / NH_4^+ in soil promoted the oxidation of NH_4^+ and thus provided electron acceptors for denitrification. That is, the enrichment of nitrate through nitrification also promotes denitrification. Based on the stable isotopes of N_2O ($\delta^{15}N$, $\delta^{18}O$, and SP), along with in vitro acetylene blockage experiments on agricultural soils fertilized with NH_4^+, Zhang et al. (2016) reported that while 50 %–70 % of N_2O was produced through nitrification, nitrifier denitrification ($NH_4^+ \rightarrow NO_2^- \rightarrow N_2O$) and/or heterotrophic denitrification ($NH_4^+ \rightarrow NO_3^- \rightarrow NO_2^- \rightarrow N_2O$) accounted for 30 %–50 % of N_2O production. Similar results have also been reported in previous studies. Although N_2O production through nitrification was simulated by fertilization with urea / NH_4^+ in various soils, denitrification also accounted for a significant portion of N_2O production (Kaushal et al., 2022; Khalil et al., 2004; Zhu et al., 2013). In addition to nitrifier and heterotrophic denitrification, N_2O produced through the anammox process ($NH_4^+ + NO_2^- \rightarrow N_2O$, Okabe et al., 2011; Tang et al., 2011; Tsushima et al., 2007) can be responsible for the reduction of NO_2^- as well. Zhu et al. (2011) found that the highest rate of anammox was comparable with that of denitrification in soils fertilized with NH_4^+ (6.2–178.8 mg N kg^{-1}). These previous experiments support our observation on the U plot that the addition of urea / NH_4^+ stimulates N_2O production through nitrifier denitrification and/or heterotrophic denitrification, and/or anammox reaction in addition to nitrification. The increased NO_3^- concentration in the U plot (13.0 ± 10.7 mg N kg^{-1}) compared with those in the NF plot (2.3 ± 0.5 mg N kg^{-1}) probably due to nitrification stimulated by the addition of NH_4^+ may be responsible for the active reduction of NO_2^-.

4.5 Stable $\Delta^{17}O$ as a natural signature for identifying N_2O production pathways

Although the $\delta^{18}O$ values of N_2O emitted from the soil were significantly higher than those of the sources of O atoms in N_2O (NO_2^-, O_2, and H_2O; Figs. 4e and 6a) due to the fractionations of oxygen isotopes during the production and/or reduction of N_2O, the $\Delta^{17}O$ values of N_2O remained within the range of these sources. This indicates that $\Delta^{17}O$ primarily reflects the pathways of N_2O production, providing information distinct from the $\delta^{18}O$ signature because $\Delta^{17}O$ is stable during the processes of biogeochemical isotope fractionation. Moreover, while N_2O emission from the forested soil did not show significant differences in $\delta^{15}N$ and $\delta^{18}O$ values between fine and rainy days due to the fractionations of nitrogen and oxygen isotopes (Fig. 4f and h), the significant difference in the $\Delta^{17}O$ values of N_2O between fine and rainy days (Fig. 4d) highlights $\Delta^{17}O$ to be a promising natural signature for identifying the pathways of N_2O production in soils.

In addition to natural soils, the stable $\Delta^{17}O$ signature is expected to be useful for identifying the pathways of N_2O production in various ecosystems, such as agricultural soils and aquatic environments, where the isotopic fractionations of nitrogen and oxygen isotopes involving biogeochemical processes are significant as well. However, to identify the pathways of N_2O production quantitatively, the uncertainties, including the β values of each reaction during N_2O production and the contributions of O atoms derived from soil H_2O during N_2O production, should be quantified precisely in the future studies.

5 Conclusions

Temporal variations in $\Delta^{17}O$ of N_2O emitted from forested soil were determined to identify the main pathway of N_2O production. Both $\Delta^{17}O$ values and fluxes of N_2O were significantly higher on rainy days compared to fine days. In addition, the $\Delta^{17}O$ values of N_2O emitted on rainy and fine days were close to those of soil NO_2^- and O_2, respectively. Because NO_2^- and O_2 were the source of O-atoms in N_2O production through denitrification and nitrification, respectively, we concluded that while nitrification dominated N_2O production on fine days, denitrification became active on rainy days, resulting in the N_2O flux increasing. In addition, the $\Delta^{17}O$ of N_2O emitted from the same soil fertilized with either Chile saltpeter or urea exhibited values that were significantly different from those of soil H_2O, implying that the contributions of O atoms derived from soil H_2O during N_2O production were minor. Furthermore, while N_2O emitted from the forested soil did not show significant differences in $\delta^{15}N$ and $\delta^{18}O$ values between fine and rainy days, the significant difference in the $\Delta^{17}O$ values of N_2O highlights $\Delta^{17}O$ to be a promising natural signature for identifying the pathways of N_2O production in soils, because $\Delta^{17}O$ is almost stable during isotope fractionation processes such as N_2O production and reduction.

Data availability. All the primary data are presented in the Supplement.

Supplement. The supplement related to this article is available online at https://doi.org/10.5194/bg-22-4333-2025-supplement.

Author contributions. WD, UT, and FN designed the study. WD, TH, WR, MI, HX, and YK performed the field observations. WD, UT, TS and FN determined the concentrations and isotopic compositions of the samples. WD, TS, FN, and UT performed data analysis.

Competing interests. The contact author has declared that none of the authors has any competing interests.

Disclaimer. Publisher's note: Copernicus Publications remains neutral with regard to jurisdictional claims made in the text, published maps, institutional affiliations, or any other geographical representation in this paper. While Copernicus Publications makes every effort to include appropriate place names, the final responsibility lies with the authors.

Acknowledgements. We thank the anonymous referees for their valuable remarks on an earlier version of this paper. We are grateful to the members of the Biogeochemistry Group at Nagoya University for their valuable support throughout this study.

Financial support. This research has been supported by the Grant-in-Aid for Scientific Research from the Ministry of Education, Culture, Sports, Science, and Technology of Japan (grant nos. 22H00561, 17H00780, and 22K19846); the Grant-in-Aid for Japan Society for the Promotion of Science Fellows (grant no. 23KJ1088); the Yanmar Environmental Sustainability Support Association; the River Fund of the River Foundation, Japan; the Reiwa Environmental Foundation; and the National Research Foundation of Korea Grant from the South Korean Government (MSIT; the Ministry of Science and ICT, grant nos. NRF-2021M1A5A1065425, KOPRI-PN24011).

Review statement. This paper was edited by David McLagan and reviewed by two anonymous referees.

References

Aggarwal, P. K. and Dillon, M. A.: Stable Isotope Composition of Molecular Oxygen in Soil Gas and Groundwater: A Potentially Robust Tracer for Diffusion and Oxygen Consumption Processes, Geochim. Cosmochim. Ac., 62, 577–584, https://doi.org/10.1016/S0016-7037(97)00377-3, 1998.

Anthony, T. L., Szutu, D. J., Verfaillie, J. G., Baldocchi, D. D., and Silver, W. L.: Carbon-sink potential of continuous alfalfa agriculture lowered by short-term nitrous oxide emission events, Nat. Commun., 14, 1926, https://doi.org/10.1038/s41467-023-37391-2, 2023.

Aron, P. G., Levin, N. E., Beverly, E. J., Huth, T. E., Passey, B. H., Pelletier, E. M., Poulsen, C. J., Winkelstern, I. Z., and Yarian, D. A.: Triple oxygen isotopes in the water cycle, Chem. Geol., 565, 120026, https://doi.org/10.1016/j.chemgeo.2020.120026, 2021.

Avrahami, S., Conrad, R., and Braker, G.: Effect of Soil Ammonium Concentration on N_2O Release and on the Community Structure of Ammonia Oxidizers and Denitrifiers, Appl. Environ. Microbiol., 68, 5685–5692, https://doi.org/10.1128/AEM.68.11.5685-5692.2002, 2002.

Balderston, W. L., Sherr, B., and Payne, W. J.: Blockage by acetylene of nitrous oxide reduction in *Pseudomonas perfectomarinus*, Appl. Environ. Microbiol., 31, 504–508, https://doi.org/10.1128/aem.31.4.504-508.1976, 1976.

Bateman, E. J. and Baggs, E. M.: Contributions of nitrification and denitrification to N_2O emissions from soils at different water-filled pore space, Biol. Fert. Soils, 41, 379–388, https://doi.org/10.1007/s00374-005-0858-3, 2005.

Cao, X. and Liu, Y.: Equilibrium mass-dependent fractionation relationships for triple oxygen isotopes, Geochim. Cosmochim. Ac., 75, 7435–7445, https://doi.org/10.1016/j.gca.2011.09.048, 2011.

Chen, G. C., Tam, N. F. Y., and Ye, Y.: Spatial and seasonal variations of atmospheric N_2O and CO_2 fluxes from a subtropical mangrove swamp and their relationships with soil characteristics, Soil Biol. Biochem., 48, 175–181, https://doi.org/10.1016/j.soilbio.2012.01.029, 2012.

Choudhary, M. A., Akramkhanov, A., and Saggar, S.: Nitrous oxide emissions from a New Zealand cropped soil: tillage effects, spatial and seasonal variability, Agr. Ecosyst. Environ., 93, 33–43, https://doi.org/10.1016/S0167-8809(02)00005-1, 2002.

Cliff, S. S., Brenninkmeijer, C. A. M., and Thiemens, M. H.: First measurement of the $^{18}O/^{16}O$ and $^{17}O/^{16}O$ ratios in stratospheric nitrous oxide: A mass-independent anomaly, J. Geophys. Res.-Atmos., 104, 16171–16175, https://doi.org/10.1029/1999JD900152, 1999.

Decock, C. and Six, J.: An assessment of N-cycling and sources of N_2O during a simulated rain event using natural abundance ^{15}N, Agr. Ecosyst. Environ., 165, 141–150, https://doi.org/10.1016/j.agee.2012.11.012, 2013.

Dickinson, R. E. and Cicerone, R. J.: Future global warming from atmospheric trace gases, Nature, 319, 109–115, https://doi.org/10.1038/319109a0, 1986.

Ding, W., Tsunogai, U., Nakagawa, F., Sambuichi, T., Sase, H., Morohashi, M., and Yotsuyanagi, H.: Tracing the source of nitrate in a forested stream showing elevated concentrations during storm events, Biogeosciences, 19, 3247–3261, https://doi.org/10.5194/bg-19-3247-2022, 2022.

Ding, W., Tsunogai, U., Nakagawa, F., Sambuichi, T., Chiwa, M., Kasahara, T., and Shinozuka, K.: Stable isotopic evidence for the excess leaching of unprocessed atmospheric nitrate from forested catchments under high nitrogen saturation, Biogeosciences, 20, 753–766, https://doi.org/10.5194/bg-20-753-2023, 2023.

Ding, W., Tsunogai, U., and Nakagawa, F.: Bias in calculating gross nitrification rates in forested catchments using the triple oxygen isotopic composition ($\Delta^{17}O$) of stream nitrate, Biogeosciences, 21, 4717–4722, https://doi.org/10.5194/bg-21-4717-2024, 2024.

Hattori, S., Nuñez Palma, Y., Itoh, Y., Kawasaki, M., Fujihara, Y., Takase, K., and Yoshida, N.: Isotopic evidence for seasonality of microbial internal nitrogen cycles in a temperate forested catch-

ment with heavy snowfall, Sci. Total Environ., 690, 290–299, https://doi.org/10.1016/j.scitotenv.2019.06.507, 2019.

Hirota, A., Tsunogai, U., Komatsu, D. D., and Nakagawa, F.: Simultaneous determination of $\delta^{15}N$ and $\delta^{18}O$ of N_2O and $\delta^{13}C$ of CH_4 in nanomolar quantities from a single water sample, Rapid Commun. Mass Sp., 24, 1085–1092, https://doi.org/10.1002/rcm.4483, 2010.

Hiyama, T., Kochi, K., Kobayashi, N., and Sirisampan, S.: Seasonal variation in stomatal conductance and physiological factors observed in a secondary warm-temperate forest, Ecol. Res., 20, 333–346, https://doi.org/10.1007/s11284-005-0049-6, 2005.

Homyak, P. M., Vasquez, K. T., Sickman, J. O., Parker, D. R., and Schimel, J. P.: Improving Nitrite Analysis in Soils: Drawbacks of the Conventional 2 M KCl Extraction, Soil Sci. Soc. Am. J., 79, 1237–1242, https://doi.org/10.2136/sssaj2015.02.0061n, 2015.

Ibraim, E., Wolf, B., Harris, E., Gasche, R., Wei, J., Yu, L., Kiese, R., Eggleston, S., Butterbach-Bahl, K., Zeeman, M., Tuzson, B., Emmenegger, L., Six, J., Henne, S., and Mohn, J.: Attribution of N_2O sources in a grassland soil with laser spectroscopy based isotopocule analysis, Biogeosciences, 16, 3247–3266, https://doi.org/10.5194/bg-16-3247-2019, 2019.

Kaiser, J., Röckmann, T., and Brenninkmeijer, C. A. M.: Complete and accurate mass spectrometric isotope analysis of tropospheric nitrous oxide, J. Geophys. Res.-Atmos., 108, 4476, https://doi.org/10.1029/2003JD003613, 2003.

Kaiser, J., Hastings, M. G., Houlton, B. Z., Röckmann, T., and Sigman, D. M.: Triple Oxygen Isotope Analysis of Nitrate Using the Denitrifier Method and Thermal Decomposition of N_2O, Anal. Chem., 79, 599–607, https://doi.org/10.1021/ac061022s, 2007.

Kaushal, R., Hsueh, Y.-H., Chen, C.-L., Lan, Y.-P., Wu, P.-Y., Chen, Y.-C., and Liang, M.-C.: Isotopic assessment of soil N_2O emission from a sub-tropical agricultural soil under varying N-inputs, Sci. Total Environ., 827, 154311, https://doi.org/10.1016/j.scitotenv.2022.154311, 2022.

Keeling, C. D.: The concentration and isotopic abundances of atmospheric carbon dioxide in rural areas, Geochim. Cosmochim. Ac., 13, 322–334, https://doi.org/10.1016/0016-7037(58)90033-4, 1958.

Khalil, K., Mary, B., and Renault, P.: Nitrous oxide production by nitrification and denitrification in soil aggregates as affected by O_2 concentration, Soil Biol. Biochem., 36, 687–699, https://doi.org/10.1016/j.soilbio.2004.01.004, 2004.

Kim, K.-R. and Craig, H.: Nitrogen-15 and Oxygen-18 Characteristics of Nitrous Oxide: A Global Perspective, Science, 262, 1855–1857, https://doi.org/10.1126/science.262.5141.1855, 1993.

Komatsu, D. D., Ishimura, T., Nakagawa, F., and Tsunogai, U.: Determination of the $^{15}N/^{14}N$, $^{17}O/^{16}O$, and $^{18}O/^{16}O$ ratios of nitrous oxide by using continuous-flow isotope-ratio mass spectrometry, Rapid Commun. Mass Sp., 22, 1587–1596, https://doi.org/10.1002/rcm.3493, 2008.

Kool, D. M., Wrage, N., Oenema, O., Dolfing, J., and Van Groenigen, J. W.: Oxygen exchange between (de)nitrification intermediates and H_2O and its implications for source determination of NO and N_2O: a review, Rapid Commun. Mass Sp., 21, 3569–3578, https://doi.org/10.1002/rcm.3249, 2007.

Kool, D. M., Dolfing, J., Wrage, N., and Van Groenigen, J. W.: Nitrifier denitrification as a distinct and significant source of nitrous oxide from soil, Soil Biol. Biochem., 43, 174–178, https://doi.org/10.1016/j.soilbio.2010.09.030, 2011.

Lewicka-Szczebak, D., Well, R., Köster, J. R., Fuß, R., Senbayram, M., Dittert, K., and Flessa, H.: Experimental determinations of isotopic fractionation factors associated with N_2O production and reduction during denitrification in soils, Geochim. Cosmochim. Ac., 134, 55–73, https://doi.org/10.1016/j.gca.2014.03.010, 2014.

Lewicka-Szczebak, D., Well, R., Bol, R., Gregory, A. S., Matthews, G. P., Misselbrook, T., Whalley, W. R., and Cardenas, L. M.: Isotope fractionation factors controlling isotopocule signatures of soil-emitted N_2O produced by denitrification processes of various rates, Rapid Commun. Mass Sp., 29, 269–282, https://doi.org/10.1002/rcm.7102, 2015.

Lewicka-Szczebak, D., Jansen-Willems, A., Müller, C., Dyckmans, J., and Well, R.: Nitrite isotope characteristics and associated soil N transformations, Sci. Rep., 11, 5008, https://doi.org/10.1038/s41598-021-83786-w, 2021.

Lin, W., Ding, J., Li, Y., Zhang, W., Ahmad, R., Xu, C., Mao, L., Qiang, X., Zheng, Q., and Li, Q.: Partitioning of sources of N_2O from soil treated with different types of fertilizers by the acetylene inhibition method and stable isotope analysis, Europ. J. Soil Sci., 70, 1037–1048, https://doi.org/10.1111/ejss.12782, 2019.

Luo, J., Ledgard, S. F., and Lindsey, S. B.: Nitrous oxide emissions from application of urea on New Zealand pasture, New Zeal. J. Agr. Res., 50, 1–11, https://doi.org/10.1080/00288230709510277, 2007.

Lyu, S.: Variability of δ^2H and $\delta^{18}O$ in Soil Water and Its Linkage to Precipitation in an East Asian Monsoon Subtropical Forest Plantation, Water, 13, 2930, https://doi.org/10.3390/w13202930, 2021.

Mathieu, O., Hénault, C., Lévêque, J., Baujard, E., Milloux, M.-J., and Andreux, F.: Quantifying the contribution of nitrification and denitrification to the nitrous oxide flux using ^{15}N tracers, Environ. Pollut., 144, 933–940, https://doi.org/10.1016/j.envpol.2006.02.005, 2006.

Matsuhisa, Y., Goldsmith, J. R., and Clayton, R. N.: Mechanisms of hydrothermal crystallization of quartz at 250 °C and 15 kbar, Geochim. Cosmochim. Ac., 42, 173–182, https://doi.org/10.1016/0016-7037(78)90130-8, 1978.

McIlvin, M. R. and Altabet, M. A.: Chemical Conversion of Nitrate and Nitrite to Nitrous Oxide for Nitrogen and Oxygen Isotopic Analysis in Freshwater and Seawater, Anal. Chem., 77, 5589–5595, https://doi.org/10.1021/ac050528s, 2005.

McKenney, D. J., Wade, D. L., and Findlay, W. I.: Rates of N_2O evolution from N-fertilized soil, Geophys. Res. Lett., 5, 777–780, https://doi.org/10.1029/GL005i009p00777, 1978.

Michalski, G., Böhlke, J. K., and Thiemens, M.: Long term atmospheric deposition as the source of nitrate and other salts in the Atacama Desert, Chile: New evidence from mass-independent oxygen isotopic compositions, Geochim. Cosmochim. Ac., 68, 4023–4038, https://doi.org/10.1016/j.gca.2004.04.009, 2004.

Miller, M. F.: Isotopic fractionation and the quantification of ^{17}O anomalies in the oxygen three-isotope system: an appraisal and geochemical significance, Geochim. Cosmochim. Ac., 66, 1881–1889, https://doi.org/10.1016/S0016-7037(02)00832-3, 2002.

Mulvaney, R. L. and Kurtz, L. T.: A New Method for Determination of ^{15}N-Labeled Nitrous Oxide, Soil Sci. Soc. Am. J., 46, 1178–1184, https://doi.org/10.2136/sssaj1982.03615995004600060012x, 1982.

Nakagawa, F., Tsunogai, U., Obata, Y., Ando, K., Yamashita, N., Saito, T., Uchiyama, S., Morohashi, M., and Sase, H.: Export flux of unprocessed atmospheric nitrate from temperate forested catchments: a possible new index for nitrogen saturation, Biogeosciences, 15, 7025–7042, https://doi.org/10.5194/bg-15-7025-2018, 2018.

Okabe, S., Oshiki, M., Takahashi, Y., and Satoh, H.: N_2O emission from a partial nitrification–anammox process and identification of a key biological process of N_2O emission from anammox granules, Water Res., 45, 6461–6470, https://doi.org/10.1016/j.watres.2011.09.040, 2011.

Opdyke, M. R., Ostrom, N. E., and Ostrom, P. H.: Evidence for the predominance of denitrification as a source of N_2O in temperate agricultural soils based on isotopologue measurements, Global Biogeochem. Cy., 23, GB4018, https://doi.org/10.1029/2009GB003523, 2009.

Ostrom, N. E., Pitt, A., Sutka, R., Ostrom, P. H., Grandy, A. S., Huizinga, K. M., and Robertson, G. P.: Isotopologue effects during N_2O reduction in soils and in pure cultures of denitrifiers, J. Geophys. Res.-Biogeo., 112, G02005, https://doi.org/10.1029/2006JG000287, 2007.

Pack, A. and Herwartz, D.: The triple oxygen isotope composition of the Earth mantle and understanding $\Delta^{17}O$ variations in terrestrial rocks and minerals, Earth Planet. Sc. Lett., 390, 138–145, https://doi.org/10.1016/j.epsl.2014.01.017, 2014.

Sambuichi, T., Tsunogai, U., Kura, K., Nakagawa, F., and Ohba, T.: High-precision $\Delta'^{17}O$ measurements of geothermal H_2O and MORB on the VSMOW-SLAP scale: evidence for active oxygen exchange between the lithosphere and hydrosphere, Geochem. J., 55, e25–e33, https://doi.org/10.2343/geochemj.2.0644, 2021.

Sambuichi, T., Tsunogai, U., Ito, M., and Nakagawa, F.: First Measurements on Triple Oxygen Isotopes of Dissolved Inorganic Phosphate in the Hydrosphere, Environ. Sci. Technol., 57, 3415–3424, https://doi.org/10.1021/acs.est.2c08520, 2023.

Sharp, Z. D. and Wostbrock, J. A. G.: Standardization for the Triple Oxygen Isotope System: Waters, Silicates, Carbonates, Air, and Sulfates, Rev. Mineral. Geochem., 86, 179–196, https://doi.org/10.2138/rmg.2021.86.05, 2021.

Sharp, Z. D., Gibbons, J. A., Maltsev, O., Atudorei, V., Pack, A., Sengupta, S., Shock, E. L., and Knauth, L. P.: A calibration of the triple oxygen isotope fractionation in the SiO_2–H_2O system and applications to natural samples, Geochim. Cosmochim. Ac., 186, 105–119, https://doi.org/10.1016/j.gca.2016.04.047, 2016.

Shen, Q. R., Ran, W., and Cao, Z. H.: Mechanisms of nitrite accumulation occurring in soil nitrification, Chemosphere, 50, 747–753, https://doi.org/10.1016/S0045-6535(02)00215-1, 2003.

Snider, D. M., Schiff, S. L., and Spoelstra, J.: $^{15}N/^{14}N$ and $^{18}O/^{16}O$ stable isotope ratios of nitrous oxide produced during denitrification in temperate forest soils, Geochim. Cosmochim. Ac., 73, 877–888, https://doi.org/10.1016/j.gca.2008.11.004, 2009.

Takahashi, K.: Oxygen isotope ratios between soil water and stem water of trees in pot experiments, Ecol. Res., 13, 1–5, https://doi.org/10.1046/j.1440-1703.1998.00240.x, 1998.

Tang, C.-J., Zheng, P., Wang, C.-H., Mahmood, Q., Zhang, J.-Q., Chen, X.-G., Zhang, L., and Chen, J.-W.: Performance of high-loaded ANAMMOX UASB reactors containing granular sludge, Water Res., 45, 135–144, https://doi.org/10.1016/j.watres.2010.08.018, 2011.

Thiemens, M. H. and Trogler, W. C.: Nylon Production: An Unknown Source of Atmospheric Nitrous Oxide, Science, 251, 932–934, https://doi.org/10.1126/science.251.4996.932, 1991.

Tian, H., Xu, R., Canadell, J. G., Thompson, R. L., Winiwarter, W., Suntharalingam, P., Davidson, E. A., Ciais, P., Jackson, R. B., Janssens-Maenhout, G., Prather, M. J., Regnier, P., Pan, N., Pan, S., Peters, G. P., Shi, H., Tubiello, F. N., Zaehle, S., Zhou, F., Arneth, A., Battaglia, G., Berthet, S., Bopp, L., Bouwman, A. F., Buitenhuis, E. T., Chang, J., Chipperfield, M. P., Dangal, S. R. S., Dlugokencky, E., Elkins, J. W., Eyre, B. D., Fu, B., Hall, B., Ito, A., Joos, F., Krummel, P. B., Landolfi, A., Laruelle, G. G., Lauerwald, R., Li, W., Lienert, S., Maavara, T., MacLeod, M., Millet, D. B., Olin, S., Patra, P. K., Prinn, R. G., Raymond, P. A., Ruiz, D. J., van der Werf, G. R., Vuichard, N., Wang, J., Weiss, R. F., Wells, K. C., Wilson, C., Yang, J., and Yao, Y.: A comprehensive quantification of global nitrous oxide sources and sinks, Nature, 586, 248–256, https://doi.org/10.1038/s41586-020-2780-0, 2020.

Toyoda, S., Yano, M., Nishimura, S., Akiyama, H., Hayakawa, A., Koba, K., Sudo, S., Yagi, K., Makabe, A., Tobari, Y., Ogawa, N. O., Ohkouchi, N., Yamada, K., and Yoshida, N.: Characterization and production and consumption processes of N_2O emitted from temperate agricultural soils determined via isotopomer ratio analysis, Global Biogeochem. Cy., 25, GB2008, https://doi.org/10.1029/2009GB003769, 2011.

Toyoda, S., Kuroki, N., Yoshida, N., Ishijima, K., Tohjima, Y., and Machida, T.: Decadal time series of tropospheric abundance of N_2O isotopomers and isotopologues in the Northern Hemisphere obtained by the long-term observation at Hateruma Island, Japan, J. Geophys. Res.-Atmos., 118, 3369–3381, https://doi.org/10.1002/jgrd.50221, 2013.

Toyoda, S., Yoshida, N., and Koba, K.: Isotopocule analysis of biologically produced nitrous oxide in various environments, Mass Spectrom. Rev., 36, 135–160, https://doi.org/10.1002/mas.21459, 2017.

Tsunogai, U., Ishibashi, J., Wakita, H., and Gamo, T.: Methane-rich plumes in the Suruga Trough (Japan) and their carbon isotopic characterization, Earth Planet. Sc. Lett., 160, 97–105, https://doi.org/10.1016/S0012-821X(98)00075-2, 1998.

Tsunogai, U., Hachisu, Y., Komatsu, D. D., Nakagawa, F., Gamo, T., and Akiyama, K.: An updated estimation of the stable carbon and oxygen isotopic compositions of automobile CO emissions, Atmos. Environ., 37, 4901–4910, https://doi.org/10.1016/j.atmosenv.2003.08.008, 2003.

Tsunogai, U., Kido, T., Hirota, A., Ohkubo, S. B., Komatsu, D. D., and Nakagawa, F.: Sensitive determinations of stable nitrogen isotopic composition of organic nitrogen through chemical conversion into N_2O, Rapid Commun. Mass Sp., 22, 345–354, https://doi.org/10.1002/rcm.3368, 2008.

Tsunogai, U., Komatsu, D. D., Daita, S., Kazemi, G. A., Nakagawa, F., Noguchi, I., and Zhang, J.: Tracing the fate of atmospheric nitrate deposited onto a forest ecosystem in Eastern Asia using $\Delta^{17}O$, Atmos. Chem. Phys., 10, 1809–1820, https://doi.org/10.5194/acp-10-1809-2010, 2010.

Tsunogai, U., Kamimura, K., Anzai, S., Nakagawa, F., and Komatsu, D. D.: Hydrogen isotopes in volcanic plumes: Tracers for remote temperature sensing of fumaroles, Geochim. Cosmochim. Ac., 75, 4531–4546, https://doi.org/10.1016/j.gca.2011.05.023, 2011.

Tsushima, I., Ogasawara, Y., Kindaichi, T., Satoh, H., and Okabe, S.: Development of high-rate anaerobic ammonium-oxidizing (anammox) biofilm reactors, Water Res., 41, 1623–1634, https://doi.org/10.1016/j.watres.2007.01.050, 2007.

Uechi, Y. and Uemura, R.: Dominant influence of the humidity in the moisture source region on the ^{17}O-excess in precipitation on a subtropical island, Earth Planet. Sc. Lett., 513, 20–28, https://doi.org/10.1016/j.epsl.2019.02.012, 2019.

Verhoeven, E., Barthel, M., Yu, L., Celi, L., Said-Pullicino, D., Sleutel, S., Lewicka-Szczebak, D., Six, J., and Decock, C.: Early season N_2O emissions under variable water management in rice systems: source-partitioning emissions using isotope ratios along a depth profile, Biogeosciences, 16, 383–408, https://doi.org/10.5194/bg-16-383-2019, 2019.

Wankel, S. D., Ziebis, W., Buchwald, C., Charoenpong, C., de Beer, D., Dentinger, J., Xu, Z., and Zengler, K.: Evidence for fungal and chemodenitrification based N_2O flux from nitrogen impacted coastal sediments, Nat. Commun., 8, 15595, https://doi.org/10.1038/ncomms15595, 2017.

WMO: WMO greenhouse gas bulletin (GHG Bulletin), https://library.wmo.int/records/item/68532-no-19-15-november-2023 (last access: 14 June 2025), 2023.

Wrage, N., Velthof, G. L., van Beusichem, M. L., and Oenema, O.: Role of nitrifier denitrification in the production of nitrous oxide, Soil Biol. Biochem., 33, 1723–1732, https://doi.org/10.1016/S0038-0717(01)00096-7, 2001.

Wrage, N., Lauf, J., del Prado, A., Pinto, M., Pietrzak, S., Yamulki, S., Oenema, O., and Gebauer, G.: Distinguishing sources of N_2O in European grasslands by stable isotope analysis, Rapid Commun. Mass Sp., 18, 1201–1207, https://doi.org/10.1002/rcm.1461, 2004.

Wrage, N., Groenigen, J. W. van, Oenema, O., and Baggs, E. M.: A novel dual-isotope labelling method for distinguishing between soil sources of N_2O, Rapid Commun. Mass Sp., 19, 3298–3306, https://doi.org/10.1002/rcm.2191, 2005.

Xu, H., Tsunogai, U., Nakagawa, F., Li, Y., Ito, M., Sato, K., and Tanimoto, H.: Determination of the triple oxygen isotopic composition of tropospheric ozone in terminal positions using a multistep nitrite-coated filter-pack system, Rapid Commun. Mass Sp., 35, e9124, https://doi.org/10.1002/rcm.9124, 2021.

Yan, Y., Sha, L., Cao, M., Zheng, Z., Tang, J., Wang, Y., Zhang, Y., Wang, R., Liu, G., Wang, Y., and Sun, Y.: Fluxes of CH_4 and N_2O from soil under a tropical seasonal rain forest in Xishuangbanna, Southwest China, J. Environ. Sci., 20, 207–215, https://doi.org/10.1016/S1001-0742(08)60033-9, 2008.

York, D., Evensen, N. M., Martìnez, M. L., and De Basabe Delgado, J.: Unified equations for the slope, intercept, and standard errors of the best straight line, Am. J. Phys., 72, 367–375, https://doi.org/10.1119/1.1632486, 2004.

Young, E. D., Galy, A., and Nagahara, H.: Kinetic and equilibrium mass-dependent isotope fractionation laws in nature and their geochemical and cosmochemical significance, Geochim. Cosmochim. Ac., 66, 1095–1104, https://doi.org/10.1016/S0016-7037(01)00832-8, 2002.

Yu, L., Harris, E., Lewicka-Szczebak, D., Barthel, M., Blomberg, M. R. A., Harris, S. J., Johnson, M. S., Lehmann, M. F., Liisberg, J., Müller, C., Ostrom, N. E., Six, J., Toyoda, S., Yoshida, N., and Mohn, J.: What can we learn from N_2O isotope data? – Analytics, processes and modelling, Rapid Commun. Mass Sp., 34, e8858, https://doi.org/10.1002/rcm.8858, 2020.

Zhang, W., Li, Y., Xu, C., Li, Q., and Lin, W.: Isotope signatures of N_2O emitted from vegetable soil: Ammonia oxidation drives N_2O production in NH_4^+-fertilized soil of North China, Sci. Rep., 6, 29257, https://doi.org/10.1038/srep29257, 2016.

Zhu, G., Wang, S., Wang, Y., Wang, C., Risgaard-Petersen, N., Jetten, M. S., and Yin, C.: Anaerobic ammonia oxidation in a fertilized paddy soil, ISME J., 5, 1905–1912, https://doi.org/10.1038/ismej.2011.63, 2011.

Zhu, X., Burger, M., Doane, T. A., and Horwath, W. R.: Ammonia oxidation pathways and nitrifier denitrification are significant sources of N_2O and NO under low oxygen availability, P. Natl. Acad. Sci. USA, 110, 6328–6333, https://doi.org/10.1073/pnas.1219993110, 2013.

Zou, Y., Hirono, Y., Yanai, Y., Hattori, S., Toyoda, S., and Yoshida, N.: Rainwater, soil water, and soil nitrate effects on oxygen isotope ratios of nitrous oxide produced in a green tea (*Camellia sinensis*) field in Japan, Rapid Commun. Mass Sp., 29, 891–900, https://doi.org/10.1002/rcm.7176, 2015.